Inactivation of phosphodiesterase-4B gene in rat nucleus accumbens shell by CRISPR/Cas9 modulates the motivation to chronically self-administer nicotine

Burt M Sharp[1]*, Qin Jiang[1], Panjun Kim[2] and Hao Chen[2]

Department of Genetics, Genomics and Informatics[1]
Department of Pharmacology, Addiction Science and Toxicology[2]
College of Medicine
University of Tennessee Health Science Center, Memphis, Tennessee

* Correspondence: labsharp1@gmail.com

Abstract

Large scale human genome wide association studies (GWAS) have identified a growing pool of genes associated with cigarette smoking. One of the most prominent, phosphodiesterase-4B (PDE4B), has been associated with multiple smoking phenotypes. Although PDE4B modulates the half-life of neuronal cAMP, its precise role in smoking behaviors is unknown. To address this knowledge gap, we inactivated *PDE4B* in bilateral medial nucleus accumbens shell (NAcs) neurons by injecting AAV containing a specific gRNA in female transgenic Cas9+ Long Evans rats These rats then were given 23-hour chronic access to nicotine intravenous self-administration (IVSA) under a schedule of increasing fixed ratios (FR). With the increased effort required at FR7, nicotine SA (i.e. active presses and drug infusions) declined significantly in controls, whereas it was maintained in the mutagenized group. A progressive ratio (PR) study also showed significantly greater cumulative nicotine infusions in the mutant group. Hence, we hypothesized that enhanced PDE4B protein activity would reduce nicotine IVSA. A positive allosteric modulator, 2-(3-(4-chloro-3-fluorophenyl)-5-ethyl-1H-1,2,4-triazol-1-yl)-N-(3,5-dichlorobenzyl)aceta-mide (MR-L2), was microinfused into NAcs bilaterally at FR3 or FR5; in both cohorts, MR-L2 acutely reduced nicotine IVSA. In summary, these studies show that the activity of PDE4B regulates the capacity of NAcs to maintain nicotine IVSA in face of the cost of increasing work. This finding and the results of the PR study indicate that PDE4B affects the motivation to obtain nicotine. These studies provide insight into the motivational effects of NAcs PDE4B that may impact the smoking behaviors mapped in human GWAS.

Introduction

Large scale human genome wide association studies (GWAS) have identified a growing pool of genes associated with cigarette smoking behaviors (M. Liu et al. 2019; Saunders et al. 2022). A study of more than 1.2 million individuals in the British Biobank identified phosphodiesterase-4B (PDE4B) as one of only three genes independently associated with multiple smoking phenotypes including initiation of regular smoking, age of regular smoking, amount smoked (cigarettes/day), and smoking cessation (M. Liu et al. 2019; Saunders et al. 2022). Recently, meta-analysis of a GWAS involving 60 ancestrally diverse cohorts, comprised of 3.4 million individuals, found seven distinct single nucleotide polymorphisms (SNPs) in an intron of phosphodiesterase-4B (PDE4B) - each significantly associated with smoking initiation across ancestral groups (Saunders et al. 2022). As specific genes associated with tobacco smoking are confirmed by independent human GWAS, understanding the functional significance of specific genes has become increasingly important in the rational selection of novel therapeutic targets to substantially improve the success of smoking cessation (Zhu et al. 2012; Saunders et al. 2022).

PDE4B belongs to a large multi-gene family of PDE isoenzymes that regulate cyclic nucleotide homeostasis in multiple intracellular compartments (Francis, Blount, and Corbin 2011). PDE4B is one of four PDE4 isoenzymes (A,B,C,D) encoded by four genes that specifically catalyze the dephosphorylation of cyclic AMP (cAMP), selectively limiting the half-life of cAMP-dependent signaling by signaling complexes involved in specific cellular processes (Conti et al. 2003; Houslay 2010). Therefore, the PDE4B expressed in nucleus accumbens (NAc) (Polesskaya, Smith, and Fryxell 2007) the brain region mediating the motivation to take drugs including nicotine (Scofield et al. 2016) is most likely a critical regulator of specific signaling pathways controlling the activation of median spiny neurons (MSNs) in NAc.

The neural circuitry of NAc, largely comprised of MSNs, functions as the brain interface mediating the motivation for goal directed behaviors by integrating information from cortical and limbic inputs with outputs to brain regions involved in goal-directed behaviors (e.g., ventral pallidum). By regulating the half-life of cAMP associated with signaling complexes in MSNs and other neurons, PDE4B affects the activity of key downstream signaling molecules including protein kinase A (PKA), dopamine and cAMP-regulated phosphoprotein (DARPP-32), and cAMP-response element binding protein (CREB) (Svenningsson, Nairn, and Greengard 2005; Campbell et al. 2017). These signaling molecules modulate the excitability of MSNs (Dong et al. 2006; Onn, Fienberg, and Grace 2003; Perez, White, and Hu 2006). Signaling in this pathway (i.e., cAMP/PKA/DARPP-32/CREB) is activated by dopamine receptors (D1R), in response to dopamine release induced by nicotine and other drugs of abuse, and inhibited by D2R; these dopamine receptor (DaR) subtypes are differentially expressed by two types of MSNs (Nishi, Snyder, and Greengard 1997; Yan et al. 1999; Hamada et al. 2005).

The effects of modulating PDE4B activity on operant intravenous self-administration (IVSA) of nicotine are unknown. Based on human GWAS that have demonstrated the association of PDE4B with human smoking behavior (M. Liu et al. 2019; Saunders et al. 2022), we addressed the role of PDE4B in operant nicotine IVSA by using a well-established rat model of virtually unlimited chronic access to the drug (Valentine et al. 1997; Yu and Sharp 2015). We sought to disrupt PDE4B gene expression in medial NAc shell (NAcs) neurons, by *in vivo* genome editing using virally delivered gRNA targeting all transcripts of PDE4B in transgenic rats containing CRISPR/Cas9 (Bäck et al. 2019). To accomplish this and to selectively target neurons controlling motivation that project to ventral pallidum, rats received bilateral medial NAcs microinjections of adeno-associated virus (AAV) containing the PDE4B gRNA. In retrograde transport studies, we had previously shown that medial NAcs neurons project to ventral pallidum (Chen et al. 2011). Additional experiments were designed to enhance the activity of PDE4B protein in NAc by administering a positive allosteric modulator (PAM) specific for PDE4 long isoenzymes, which contain two upstream conserved regulatory regions (i.e., UCR1 and UCR2) (Houslay 2010; Omar et al. 2019). This PAM, 2-(3-(4-chloro-3-fluorophenyl)-5-ethyl-1H-1,2,4-triazol-1-yl)-N-(3,5-dichlorobenzyl)-aceta -mide (MR-L2), targets UCR1 and has been shown to reduce cellular cAMP levels and PKA signaling (Houslay 2010; Omar et al. 2019). We found that inactivating the PDE4B gene in NAcs neurons by CRISPR/Cas9-induced mutation increased the motivation to obtain nicotine as the FR requirement increased (i.e., number of operant lever presses required to obtain a single i.v. infusion of nicotine), whereas administration of MR-L2 had the opposite effect - decreasing the motivation to obtain nicotine.

Methods

Materials, Animals and Breeding

Heterozygous loxP-STOP-loxP Cas9+ female outbred Long Evans rats, originally obtained from Professor Aron Geurts, Medical College of Wisconsin, and developed by Brandon K. Harvey Ph.D. at NIH (Bäck et al. 2019) were used in all experiments. A breeding colony of these rats was maintained in our vivarium using wildtype Long Evans rats purchased from Charles River Laboratories, and genotyped by Transnetyx (Memphis, TN) to identify Cas9+ females. 2-(3-(4-chloro-3-fluorophenyl)-5-ethyl-1H-1,2,4-triazol-1-yl)-N-(3,5-di- chlorobenzyl)acetamide (MR-L2) was purchased from Targetmol Chemicals Inc., Wellesley Hills, MA (CAS #2374703-19-0). A stock solution of MR-L2 (5.0 mM) was prepared in 100% DMSO and then diluted with a 20% solution of Sulfobutylether-β-Cyclodextrin (SBE-β-CD; CAS #182410-00-0; Targetmol Chemicals Inc.) in sterile saline.

Identification of an effective gRNA complementary to rat PDE4

In consultation with our laboratories, Applied Biological Materials Inc., Richmond, BC, Canada, designed three gRNAs to rat PDE4B, using their proprietary software and generated viral vectors (10^{12} GC/ml) with the following structure: pAAV-hSyn-Kozak-iCre-P2A-mClover3-U6-gRNA. Each was tested by microinfusion (400nl) bilaterally into rat prefrontal cortex (PFC; AP 2.95, ML1.31 or ML -1.31, DV 3.17, 10 degree), followed by: sampling of PFC from 4-5 coronal tissue sections (100 μm), based on fluorescence intensity of the accompanying mClover3 expressed by the AAV-gRNA construct in sentinel tissue sections; genomic DNA extraction from a region surrounding the gRNA injection site; and PCR amplification (5' primer: gacagcaaaagtcacatgcag; 3': gaacaaatggggccttaaca). The PCR product was then sequenced on the Illumina platform to obtain single end 150 bp reads. CRISPRpic (Lee et al. 2020) was used to analyze the sequencing data in order to identify mutations, including deletions, insertions, complex deletions, and substitutions. Only one gRNA, TGCATGTGAGGGGCCGATTA, effectively mutated the PDE4B DNA sequence. This gRNA is located on chr 5:122128512-122128531 (Rnor6.0) and chr5:117359381-117359400 (mRatBN7.2).

Stereotaxic surgery

The same procedure was used for (i) *in vivo* CRISPR/Cas9-dependent mutagenesis of neuronal PDE4B genomic DNA in nucleus accumbens shell (NAcs) or (ii) implantation of guide cannulae into NAcs for delivery of MR-L2.

Female Cas9+ LE rats, 180-200 g b.wt., were anesthetized by inhalation with 2% isoflurane and microinfused (200nl/side over 10 min; needle withdrawn 5 min, thereafter) with the aforementioned AAV or control construct (AAV-hU6 -GLuc219-gRNA-EF1α-EGFP-KASH; 3.68E+12 GC/ml, kindly provided by Dr. Brandon Harvey, NIDA IRP) targeted bilaterally to medial NAcs at AP 1.8; ML 1.4 or -1.4; DV 6.7; 5 degree. For administration of MR-L2 during operant nicotine IVSA, rats were equipped with guide cannulae implanted in medial NAcs bilaterally (AP 1.8; ML 1.4 or -1.4; DV

6.7; Angle 5 degree) and affixed to the skull with screws and dental cement. Ten days after stereotaxic surgery, under general anesthesia, a jugular vein cannula was implanted and tunneled subcutaneously to a button affixed to a small incision on the back, to which a spring-loaded tether was attached within the operant chamber for delivery of nicotine.

Access to virtually unlimited operant nicotine SA

As previously described, rats are individually housed in operant chambers, beginning 3 days after jugular surgery, and given extended access to nicotine SA (23h/day, 7 days/week) without food deprivation and prior training (Valentine et al. 1997; Yu and Sharp 2015). The operant chamber contained two horizontal levers; during IVSA sessions, a green cue light above each lever signaled that nicotine was available. Lever presses were recorded and syringe pumps were controlled by computers and interfaces, using GS3 software (Coulbourn Instruments, Allentown, PA). Nicotine IVSA started immediately upon initiation of the dark cycle (at 10 AM for 12 hours). Pressing the active lever elicited a jugular vein injection of nicotine solution (0.03 mg/kg per 50 µl/0.81 s, free base, pH 7.2–7.4). To prevent a nicotine overdose, the green cue lights were extinguished and nicotine was unavailable for 7s after each injection of nicotine. Pressing the inactive lever had no programmed consequence. The final hour of the 12 h lights-on cycle (i.e., 9:00–10:00 AM) was reserved for animal husbandry, nicotine solution refreshing, and data recording. The patency of jugular catheters was checked periodically by brevital injection (0.2 ml; JHP pharmaceuticals, Rochester, MI). Rats with occluded catheters were excluded from further study.

Experiment 1: Increasing fixed ratio (FR) required to obtain nicotine in rats with bilateral PDE4B mutations in medial NAcs vs. controls.

Stable nicotine intake in daily 23 hour sessions was achieved within 10 days of initiating nicotine IVSA at FR1 (1 active lever press triggered 1 nicotine infusion); thereafter, the FR requirement was advanced based on the following schedule: FR2, 5 days; FR3, 5 days; FR5, 7 days; FR7, 7 days. Following the behavioral experiment, cardiac perfusion under lethal isoflurane inhalation was performed with 4% paraformaldehyde followed by removal of brains and dehydration in 30% sucrose for 2 days. Coronal cryostat sections (100 µm) were obtained for fluorescence microscopy (excitation, 505nm; emission, 515nm).

Experiment 2: Effects of bilateral NAcs infusions of MR-L2 vs. vehicle control during operant nicotine IVSA at increasing FR requirements.

The FR schedule for these studies was: FR1, 10 days; FR2, 5 days, FR3, 5 days, FR5, 9 days. MR-L2 or vehicle was administered on day 4 of FR3 in one group and on day 8 of FR5 in a second, independent group of rats. During the final hour of lights-on, microinfusion needles were inserted into guide cannulae while rats were briefly anesthetized with 2% isoflurane; anesthesia ceased, MR-L2 (300 nl; $2x10^{-4}$ M in 1:20 dilution: DMSO in 20% SBE-β-CD) or vehicle (1:20 of DMSO in 20% SBE-β-CD) was microinfused (25 nl/min over 12 min) into NAcs, and needles were removed 5 min later. Rats were returned to their home operant chambers 20 min later, the dark phase of the light cycle was initiated, and nicotine was immediately available. Following the

experiment, brains were removed from rats treated with lethal inhalation isoflurane + thoracotomy. Brains were flash frozen and maintained at -20℃ until cryostat sections (50 μm) were obtained to identify the locations of guide cannulae.

Data Analysis and Statistics

Active lever presses and nicotine infusions at FR7 were compared in AAV experimental and control groups, as were infusions obtained during a PR (progressive ratio) study. For the studies of MR-L2, daily active and inactive lever presses and infusions were compared throughout FR3 or FR5 in two independent experiments. Additionally, cumulative active presses and infusions were divided into consecutive 3-hour bins on the day that MR-L2 or vehicle was injected in each of the two experiments. These data were expressed as a percentage of the mean value for the corresponding time bins recorded during the 3 preceding days.

Behavioral data were analyzed by repeated measures 2-way ANOVA, using R package, with either day of lever press or nicotine infusion designated as a within-subject factors and treatment designated as a between-subject factor. TukeyHSD test was used for *posthoc* testing. PR data and time binned data were compared between treatment groups by t-test; P values were Bonferroni-adjusted for multiple comparisons. Data were expressed as mean ± SEM. Statistical significance was assigned at $p < 0.05$.

Results

Using the CRISPR/Cas9 technology targeted to neurons by neuron-specific expression of iCre and, therefore, Cas9, a gRNA specific for rat PDE4B exon 9, common to all PDE4B transcripts, generated several types of mutations (Figure 1) detected in heterogeneous tissue dissected from the medial NAc shell after AAV injection. For each of these mutants, the data are expressed as fold change compared to control tissue: insertions, deletions and complex changes in PDE4B were approximately 95, 75 and 20-fold, respectively, more common in tissue from NAcs treated *in vivo* with PDE4B-gRNA (i.e, pAAV8-hSyn-Kozak-iCre-P2A-mClover3-U6-gRNA) compared to control (AAV-hU6 -GLuc219-gRNA-EF1α-EGFP-KASH). The fold-change depended on the dose of AAV injected. Insertions, for example, were reduced from 95-fold to 13-fold greater than control by decreasing the dose 10-fold.

Representative photomicrographs of mClover fluorescence from one rat brain at AP 1.7 and 2.2 are shown in Figure 2. Abundant fluorescence, detected 45 days after injection of the AAV PDE4B-gRNA construct and completion of a trial of nicotine SA through FR7, is predominantly in nuclei within the NAc shell. Hence, Cas9-dependent mutagenesis, targeted to PDE4B by the PDE4B-gRNA, is localized to neurons largely in the medial NAc shell.

<u>Experiment 1</u>

Figure 3 shows active lever presses (upper panel) and nicotine infusions by day as FR increased from FR1 to FR7. By the final 2-3 days at FR1-5, presses and infusions were similar in the experimental (EXP) and control (CNT) groups. However, at FR7, these parameters diverged between the two treatment groups: both presses and infusions increased from the first to the final day at FR7 in the EXP group, whereas both parameters decreased over this time interval in the CNT group. Comparing the final 3 days of active lever presses at FR7 to FR5, in the EXP group FR7 was greater, whereas it was less in the CNT group. Nicotine injections were similar during the final 3 days of FR7 vs. FR5 in the EXP group, whereas injections declined in the CNT group.

Taking the average daily active press elicited by each rat during the final 3 days of FR7, we found: EXP = 403.1 ± 68.9 (mean ± SE; n=14) vs. CNT = 211.3 ± 36.5 (n=12) (P=0.028); nicotine infusions, EXP = 33.9 ± 4.6 vs. CNT = 17.9±3.7 (P=0.0134). Comparing all 7 daily FR7 responses for EXP vs CNT (repeated measures 2-way ANOVA) showed a significant treatment effect on injection (P=0.046), but not on active presses (P=0.081). Lastly, a progressive ratio (PR) test was conducted the day after completion of nicotine IVSA at FR7. Figure 4 shows the cumulative infusions obtained by the two treatment groups: EXP = 10.0 ± 0.5 vs. CNT = 7.7 ± 0.7 (P=0.018). In summary, region-specific mutagenesis of PDE4B in medial NAcs sustained lever pressing to self-administer i.v. nicotine despite the high FR requirement (i.e. FR7), whereas active presses and nicotine infusions declined in the CNT group. This difference is reinforced by the significant difference in infusions obtained during the PR test - an index of motivation to obtain nicotine.

Experiment 2

Rats with bilateral NAcs guide cannula implants self-administered nicotine under a schedule of increasing FR. Figure 5 is a schematic showing the NAcs positions of the injection needle tips used to administer MR-L2 ($2x10^{-4}$ M, 300nl/side) on day 6 of the 7-day FR3 schedule. Almost all injection tips were tightly localized to medial NAcs.

Figure 6 shows the effect of MR-L2 on active presses and infusions at FR3 in EXP (upper panel) and CNT (i.e., received DMSO-SBE) groups. MR-L2 significantly reduced active lever presses on day 6 in EXP, but not in CNT: effect of treatment, F=0.49, P=0.5; day, F=10.35, P=0.0054; treatment x day, F=9.60, P=0.0069 (repeated measures 2-way ANOVA). *Post-hoc* analysis showed that active presses on days 3-5 were greater than day 6 in the EXP (P=0.029, TukeyHSD), but not CNT (P=0.99) group. We found similar differences for nicotine infusions between the two treatment groups: treatment, F=0.69, P=0.42; day, F=9.28, P=0.0077; treatment x day, F=9.44, P=0.0073; infusions on days 3-5 > day 6 in EXP (P=0.033; TukeyHSD), but not CNT (P=0.99).

We further analyzed the effects of MR-L2 by generating time bins containing all active presses elicited or infusions obtained within time intervals 0-3, 3-6, 6-9, and 9-12 hours after administration of MR-L2. These data were normalized by the average value for each time bin recorded on days 3-5. Figure 7 shows that the greatest effects of MR-L2 (EXP) vs. vehicle (CNT) on active presses and infusions occurred between 3-6 hours after dosing: effects of treatment at 3-6 hours post dose, P=0.0048 and 0.0012, respectively; all other time bins, P>0.05 (Bonferroni-adjusted P values).

Figure 8 is a schematic showing the NAcs positions of the injection needle tips used to administer MR-L2 ($2x10^{-4}$ M, 300nl/side) on day 8 of the 9-day FR5 schedule. The effects of MR-L2 on active presses and nicotine infusions at FR5 in EXP (upper panel) and CNT (i.e., DMSO-SBE) groups are shown in Figure 9. MR-L2 significantly reduced active presses on day 8 in EXP, but not in CNT: effect of treatment, F=0.014, P=0.91; day, F=22.61, P=8.58e-05; treatment x day, F=2.06, P=0.16 (repeated measures 2-way ANOVA). *Post-hoc* analysis showed that active presses on days 5-7 were greater than day 8 in the EXP (P=0.0071, Tukey), but not CNT (P=0.43) group. We found similar differences for nicotine infusions between the two treatment groups: treatment, F=0.088, P=0.77; day, F=16.22, P=0.00053; treatment x day, F=3.10, P=0.091; infusions on days 5-7 > day 8 in EXP (P=0.0029; Tukey), but not CNT (P=0.65).

Figure 10 shows the time bins for active presses (upper panel) and nicotine infusions obtained after administration of MR-L2 at FR5. A significant effect of treatment group was found for both presses and infusions: F=5.37, P=0.030 and F=4.84, P=0.038, respectively (repeated measures 2-way ANOVA); neither bin time nor treatment x time were significant (P > 0.05). *Post-hoc* tests were not significant.

Discussion

Although human GWAS have implicated PDE4B in multiple stages of smoking behavior (M. Liu et al. 2019; Saunders et al. 2022), the mechanism(s) underlying these effects are unknown. We hypothesized that reducing the function of PDE4B in NAcs neurons by CRISPR/Cas9 gene inactivation and enhancing the catabolic activity of the protein using MR-L2, a positive allosteric modulator, would provide insight into the role of PDE4B in nicotine SA under a schedule of increasing FR. Indeed, selective modulation of PDE4B by administration of the gRNA or MR-L2 into medial NAcs demonstrated significant and opposite effects on the maintenance of nicotine IVSA in face of increasing FR requirements. Mutagenesis of PDE4B by selective deletions and insertions in an exon specific for PDE4B maintained nicotine IVSA at high FR (i.e., FR7) compared to the declining IVSA observed in controls. Conversely, positive allosteric modulation of PDE4B rapidly reduced nicotine SA at FR3 and FR5; these FRs were otherwise well tolerated in controls.

These observations were made in rats that received microinfusions of an AAV construct into NAcs bilaterally - a construct designed to specifically mutate PDE4B only in neurons. We tested our hypothesis in the NAcs because of its critical role in operant nicotine SA (Corrigall et al. 1992; Scofield et al. 2016) and the relatively high concentration of PDE4B identified in this region (Polesskaya, Smith, and Fryxell 2007). NAc is the brain interface that integrates inputs from mesocorticolimbic regions, which transmit cognitive, emotive and reward-related information from these regions to NAc MSN. Monosynaptic inputs from regions such as frontal cortex, hippocampus and basolateral/basomedial amygdala (Li et al. 2018), activate MSNs via glutamatergic projections. Additionally, nicotine-induced dopamine release from the ventral tegmental area to MSN modulates the activation of MSN (C. Liu, Goel, and Kaeser 2021). The NAc circuitry generates MSN outputs to regions such as ventral pallidum, which engage the brain circuitry involved in goal directed behaviors (Leung and Balleine 2013; Fujimoto et al. 2019).

The high behavioral costs necessary to obtain rewards in certain operant paradigms are surmounted by increasing NAc neuronal activity (Hauber and Sommer 2009). In high-cost trials, subsets of MSN fire prior to the initiation of behavioral responding and remain active until the reward is obtained, whereas the duration of responding is shorter when the cost is less (Day, Jones, and Carelli 2011). The costs of these predictably large responses are encoded by differences in phasic dopamine signaling to MSN (Day et al. 2010). Dynamic changes in moment-to-moment dopamine release are critical to these cost-related decisions (Salamone and Correa 2002; Hamid et al. 2016) involved in motivated behavior to obtain conditioned rewards. Based on the results of PDE4B mutagenesis, we hypothesize that the high cost of obtaining nicotine reward at FR7 is not met by increased MSN activity driven by enhanced dopamine release unless dopamine signaling is further amplified by molecular changes in the neuronal landscape, such as those induced by reducing the function of PDE4B in neurons.

PDE4B interacts with compartmentalized signaling complexes and modulates dopamine signaling by regulating the half-life of cAMP synthesized following D1R activation (Francis, Blount, and Corbin 2011; Hamid et al. 2016). Additionally, glutamatergic signaling to MSN AMPA receptors is modulated by D1R/cAMP/PKA (Chao et al. 2002; Anderson et al. 2008; Sun et al. 2008). The duration and level of cAMP signaling determines the activity of downstream signaling moieties such as PKA, DARPP-32, PP1a and CREB (Svenningsson, Nairn, and Greengard 2005; Campbell et al. 2017), which are involved in regulating the excitation of MSN (Dong et al. 2006; Perez, White, and Hu 2006) and in regulation of the transcriptional landscape (Vialou et al. 2012; Kronman et al. 2019; Lardner et al. 2021). Hence, PDE4B sits at a critical juncture - impacting both the acute and chronic activation of MSN.

The acute effects of modulating PDE4B activity and, thereby, MSN excitation are exemplified by the experiments with MR-L2. We observed the effects of this compound in rats self-administering nicotine at FR3 by 3 hours after infusion into NAcs (the administration protocol, which tended to reduce nicotine SA just after delivery of the drug, obviated detecting the effect of MR-L2 earlier), and the effects waned by 6 hours. Since positive allosteric modulation of PDE4B attenuates cAMP signaling, we would expect it to reduce nicotine and dopamine-dependent excitation of MSN (Omar et al. 2019). Indeed, in two separate experiments, MR-L2 reduced active lever presses and nicotine intake at both FR3 and FR5.

Conversely, chronic down-regulation of PDE4B protein, due to disruption of gene expression by induction of deletions and insertions in a coding region, resulted in the maintenance of nicotine IVSA (i.e., active presses and nicotine intake) despite high FR demand - which reduced IVSA in controls. We would expect chronic downregulation to have more complex effects on MSN function than acute administration of a drug such as MR-L2. cAMP signaling would be tonically enhanced, thus increasing nicotine and dopamine-dependent excitation of MSN. Additionally, resetting the transcriptional landscape and the downstream expression of neuronal proteins in multiple pathways would likely produce a myriad of changes in MSN function and in behavior that remain to be delineated. For example, *in vivo* transfection of constitutively active CREB has been shown to amplify the excitability of MSN (Dong et al. 2006).

The DaR subtypes (i.e. D1R and D2R) differentially expressed by two types of NAc MSNs (Nishi, Snyder, and Greengard 1997; Yan et al. 1999; Hamada et al. 2005) have opposite effects on cAMP synthesis (Beaulieu and Gainetdinov 2011). Activation of D1R induces adenylate cyclase to synthesize cAMP, whereas D2R inhibits this enzyme (Beaulieu and Gainetdinov 2011). Therefore, increased PDE4B activity would diminish D1R-dependent cAMP signaling and the activation of D1R-MSN; conversely, increased PDE4B activity would most likely amplify the inhibitory effect of dopamine on MSN that express D2R. Hence, PDE4B modulates both the activation and inhibition of MSN, depending in large part on the expression of D1R vs. D2R (Nishi, Snyder, and Greengard 1997; Yan et al. 1999).

The effects of reducing the expression of PDE4B by CRISPR/Cas9 gene editing and enhancing the catabolic activity of the protein using MR-L2 depend on the subtype of MSN: a knock-down of the PDE4B gene would enhance D1R-dependent signaling and activation of D1R-MSN, whereas it would diminish the inhibitory effect of D2R signaling and reduce the inhibition of D2R-MSN by dopamine. Conversely, MR-L2 would be expected to reduce D1R-dependent signaling and increase D2R signaling. The relative role of each DaR-MSN subtype in determining the behavioral outcomes observed in this study are unknown. Both both subtypes of NAc MSN appear to be involved in reward and aversion (Bin Saifullah et al. 2018; Soares-Cunha et al. 2020; Yao et al. 2021), depending in part on the duration of stimulation (Soares-Cunha et al. 2020). Moreover, the motivational effects of activating a specific subtype of DaR-MSN (i.e. D2R) depend on the phase of the motivated behavior (i.e. conditioned cue vs reward consumption) (Soares-Cunha et al. 2022).

In summary, PDE4B plays a pivotal role in determining the NAcs motivational response to conditioned nicotine reinforcement. Reduced PDE4B activity, induced by CRISPR/Cas9 gene inactivation, maintains the motivation to take nicotine as the cost of work increases, whereas increased PDE4B activity impairs the motivation to take the drug. Since NAc neuronal responses to goal directed behavior are heterogenous, depending on factors such as the specific neurons sampled, the operant paradigm, and the phase of the motivated behavior (Day et al. 2010; Day, Jones, and Carelli 2011; Soares-Cunha et al. 2022), the observations made in the present study may depend in part on the area of NAcs (i.e. dorsomedial) affected by CRISPR/Cas9 and MR-L2. Nonetheless, these studies provide novel insights into the role of NAcs PDE4B in operant nicotine IVSA at increasing FR workload that contribute to understanding the heretofore unexplained GWAS associations between PDE4B and multiple stages of human smoking.

References

Anderson, Sharon M., Katie R. Famous, Ghazaleh Sadri-Vakili, Vidhya Kumaresan, Heath D. Schmidt, Caroline E. Bass, Ernest F. Terwilliger, Jang-Ho J. Cha, and R. Christopher Pierce. 2008. “CaMKII: A Biochemical Bridge Linking Accumbens Dopamine and Glutamate Systems in Cocaine Seeking.” *Nature Neuroscience* 11 (3): 344–53.

Bäck, Susanne, Julie Necarsulmer, Leslie R. Whitaker, Lamarque M. Coke, Pyry Koivula, Emily J. Heathward, Lowella V. Fortuno, et al. 2019. “Neuron-Specific Genome Modification in the Adult Rat Brain Using CRISPR-Cas9 Transgenic Rats.” *Neuron* 102 (1): 105–19.e8.

Beaulieu, Jean-Martin, and Raul R. Gainetdinov. 2011. “The Physiology, Signaling, and Pharmacology of Dopamine Receptors.” *Pharmacological Reviews* 63 (1): 182–217.

Bin Saifullah, Md Ali, Taku Nagai, Keisuke Kuroda, Bolati Wulaer, Toshitaka Nabeshima, Kozo Kaibuchi, and Kiyofumi Yamada. 2018. “Cell Type-Specific Activation of Mitogen-Activated Protein Kinase in D1 Receptor-Expressing Neurons of the Nucleus Accumbens Potentiates Stimulus-Reward Learning in Mice.” *Scientific Reports* 8 (1): 14413.

Campbell, Susan L., Thomas van Groen, Inga Kadish, Lisa High Mitchell Smoot, and Graeme B. Bolger. 2017. “Altered Phosphorylation, Electrophysiology, and Behavior on Attenuation of PDE4B Action in Hippocampus.” *BMC Neuroscience* 18 (1): 77.

Chao, Steven Z., Marjorie A. Ariano, Daniel A. Peterson, and Marina E. Wolf. 2002. “D1 Dopamine Receptor Stimulation Increases GluR1 Surface Expression in Nucleus Accumbens Neurons.” *Journal of Neurochemistry* 83 (3): 704–12.

Chen, Hao, Zhimin Liu, Suzhen Gong, Xingjun Wu, William L. Taylor, Robert W. Williams, Shannon G. Matta, and Burt M. Sharp. 2011. “Genome-Wide Gene Expression Profiling of Nucleus Accumbens Neurons Projecting to Ventral Pallidum Using Both Microarray and Transcriptome Sequencing.” *Frontiers in Neuroscience* 5 (August): 98.

Conti, Marco, Wito Richter, Celine Mehats, Gabriel Livera, Jy-Young Park, and Catherine Jin. 2003. “Cyclic AMP-Specific PDE4 Phosphodiesterases as Critical Components of Cyclic AMP Signaling.” *The Journal of Biological Chemistry* 278 (8): 5493–96.

Corrigall, W. A., K. B. Franklin, K. M. Coen, and P. B. Clarke. 1992. “The Mesolimbic Dopaminergic System Is Implicated in the Reinforcing Effects of Nicotine.” *Psychopharmacology* 107 (2-3): 285–89.

Day, Jeremy J., Joshua L. Jones, and Regina M. Carelli. 2011. “Nucleus Accumbens Neurons Encode Predicted and Ongoing Reward Costs in Rats.” *The European Journal of Neuroscience* 33 (2): 308–21.

Day, Jeremy J., Joshua L. Jones, R. Mark Wightman, and Regina M. Carelli. 2010. “Phasic Nucleus Accumbens Dopamine Release Encodes Effort- and Delay-Related Costs.” *Biological Psychiatry* 68 (3): 306–9.

Dong, Yan, Thomas Green, Daniel Saal, Helene Marie, Rachael Neve, Eric J. Nestler, and Robert C. Malenka. 2006. “CREB Modulates Excitability of Nucleus Accumbens Neurons.” *Nature Neuroscience* 9 (4): 475–77.

Francis, Sharron H., Mitsi A. Blount, and Jackie D. Corbin. 2011. “Mammalian Cyclic

Nucleotide Phosphodiesterases: Molecular Mechanisms and Physiological Functions." *Physiological Reviews* 91 (2): 651–90.
Fujimoto, Atsushi, Yukiko Hori, Yuji Nagai, Erika Kikuchi, Kei Oyama, Tetsuya Suhara, and Takafumi Minamimoto. 2019. "Signaling Incentive and Drive in the Primate Ventral Pallidum for Motivational Control of Goal-Directed Action." *The Journal of Neuroscience: The Official Journal of the Society for Neuroscience* 39 (10): 1793–1804.
Hamada, Miho, Joseph P. Hendrick, Gregory R. Ryan, Mahomi Kuroiwa, Hideho Higashi, Masatoshi Tanaka, Angus C. Nairn, Paul Greengard, and Akinori Nishi. 2005. "Nicotine Regulates DARPP-32 (dopamine- and cAMP-Regulated Phosphoprotein of 32 kDa) Phosphorylation at Multiple Sites in Neostriatal Neurons." *The Journal of Pharmacology and Experimental Therapeutics* 315 (2): 872–78.
Hamid, Arif A., Jeffrey R. Pettibone, Omar S. Mabrouk, Vaughn L. Hetrick, Robert Schmidt, Caitlin M. Vander Weele, Robert T. Kennedy, Brandon J. Aragona, and Joshua D. Berke. 2016. "Mesolimbic Dopamine Signals the Value of Work." *Nature Neuroscience* 19 (1): 117–26.
Hauber, Wolfgang, and Susanne Sommer. 2009. "Prefrontostriatal Circuitry Regulates Effort-Related Decision Making." *Cerebral Cortex* 19 (10): 2240–47.
Houslay, Miles D. 2010. "Underpinning Compartmentalised cAMP Signalling through Targeted cAMP Breakdown." *Trends in Biochemical Sciences* 35 (2): 91–100.
Kronman, Hope, Felix Richter, Benoit Labonté, Ramesh Chandra, Shan Zhao, Gabriel Hoffman, Mary Kay Lobo, Eric E. Schadt, and Eric J. Nestler. 2019. "Biology and Bias in Cell Type-Specific RNAseq of Nucleus Accumbens Medium Spiny Neurons." *Scientific Reports* 9 (1): 8350.
Lardner, Casey K., Yentl van der Zee, Molly S. Estill, Hope G. Kronman, Marine Salery, Ashley M. Cunningham, Arthur Godino, et al. 2021. "Gene-Targeted, CREB-Mediated Induction of ΔFosB Controls Distinct Downstream Transcriptional Patterns Within D1 and D2 Medium Spiny Neurons." *Biological Psychiatry* 90 (8): 540–49.
Lee, Hojoon, Howard Y. Chang, Seung Woo Cho, and Hanlee P. Ji. 2020. "CRISPRpic: Fast and Precise Analysis for CRISPR-Induced Mutations via Prefixed Index Counting." *NAR Genomics and Bioinformatics* 2 (2): lqaa012.
Leung, Beatrice K., and Bernard W. Balleine. 2013. "The Ventral Striato-Pallidal Pathway Mediates the Effect of Predictive Learning on Choice between Goal-Directed Actions." *The Journal of Neuroscience: The Official Journal of the Society for Neuroscience* 33 (34): 13848–60.
Liu, Changliang, Pragya Goel, and Pascal S. Kaeser. 2021. "Spatial and Temporal Scales of Dopamine Transmission." *Nature Reviews. Neuroscience* 22 (6): 345–58.
Liu, Mengzhen, Yu Jiang, Robbee Wedow, Yue Li, David M. Brazel, Fang Chen, Gargi Datta, et al. 2019. "Association Studies of up to 1.2 Million Individuals Yield New Insights into the Genetic Etiology of Tobacco and Alcohol Use." *Nature Genetics* 51 (2): 237–44.
Li, Zhao, Zhilong Chen, Guoqing Fan, Anan Li, Jing Yuan, and Tonghui Xu. 2018. "Cell-Type-Specific Afferent Innervation of the Nucleus Accumbens Core and Shell." *Frontiers in Neuroanatomy* 12 (October): 84.

Nishi, A., G. L. Snyder, and P. Greengard. 1997. “Bidirectional Regulation of DARPP-32 Phosphorylation by Dopamine.” *The Journal of Neuroscience: The Official Journal of the Society for Neuroscience* 17 (21): 8147–55.

Omar, Faisa, Jane E. Findlay, Gemma Carfray, Robert W. Allcock, Zhong Jiang, Caitlin Moore, Amy L. Muir, et al. 2019. “Small-Molecule Allosteric Activators of PDE4 Long Form Cyclic AMP Phosphodiesterases.” *Proceedings of the National Academy of Sciences of the United States of America* 116 (27): 13320–29.

Onn, Shao-Pii, Allen A. Fienberg, and Anthony A. Grace. 2003. “Dopamine Modulation of Membrane Excitability in Striatal Spiny Neurons Is Altered in DARPP-32 Knockout Mice.” *The Journal of Pharmacology and Experimental Therapeutics* 306 (3): 870–79.

Paxinos G, Watson C (1997) The rat brain in stereotaxic coordinates, 3rd edn. Academic Press, New York

Perez, Mariela F., Francis J. White, and Xiu-Ti Hu. 2006. “Dopamine D(2) Receptor Modulation of K(+) Channel Activity Regulates Excitability of Nucleus Accumbens Neurons at Different Membrane Potentials.” *Journal of Neurophysiology* 96 (5): 2217–28.

Polesskaya, Oksana O., Robert F. Smith, and Karl J. Fryxell. 2007. “Chronic Nicotine Doses down-Regulate PDE4 Isoforms That Are Targets of Antidepressants in Adolescent Female Rats.” *Biological Psychiatry* 61 (1): 56–64.

Salamone, John D., and Mercè Correa. 2002. “Motivational Views of Reinforcement: Implications for Understanding the Behavioral Functions of Nucleus Accumbens Dopamine.” *Behavioural Brain Research* 137 (1-2): 3–25.

Saunders, Gretchen R. B., Xingyan Wang, Fang Chen, Seon-Kyeong Jang, Mengzhen Liu, Chen Wang, Shuang Gao, et al. 2022. “Genetic Diversity Fuels Gene Discovery for Tobacco and Alcohol Use.” *Nature*, December. https://doi.org/10.1038/s41586-022-05477-4.

Scofield, M. D., J. A. Heinsbroek, C. D. Gipson, Y. M. Kupchik, S. Spencer, A. C. W. Smith, D. Roberts-Wolfe, and P. W. Kalivas. 2016. “The Nucleus Accumbens: Mechanisms of Addiction across Drug Classes Reflect the Importance of Glutamate Homeostasis.” *Pharmacological Reviews* 68 (3): 816–71.

Soares-Cunha, Carina, Ana Verónica Domingues, Raquel Correia, Bárbara Coimbra, Natacha Vieitas-Gaspar, Nivaldo A. P. de Vasconcelos, Luísa Pinto, Nuno Sousa, and Ana João Rodrigues. 2022. “Distinct Role of Nucleus Accumbens D2-MSN Projections to Ventral Pallidum in Different Phases of Motivated Behavior.” *Cell Reports* 38 (7): 110380.

Soares-Cunha, Carina, Nivaldo A. P. de Vasconcelos, Bárbara Coimbra, Ana Verónica Domingues, Joana M. Silva, Eduardo Loureiro-Campos, Rita Gaspar, Ioannis Sotiropoulos, Nuno Sousa, and Ana João Rodrigues. 2020. “Nucleus Accumbens Medium Spiny Neurons Subtypes Signal Both Reward and Aversion.” *Molecular Psychiatry* 25 (12): 3241–55.

Sun, Xiu, Michael Milovanovic, Yun Zhao, and Marina E. Wolf. 2008. “Acute and Chronic Dopamine Receptor Stimulation Modulates AMPA Receptor Trafficking in Nucleus Accumbens Neurons Cocultured with Prefrontal Cortex Neurons.” *The Journal of Neuroscience: The Official Journal of the Society for Neuroscience* 28 (16): 4216–30.

Svenningsson, Per, Angus C. Nairn, and Paul Greengard. 2005. “DARPP-32 Mediates the Actions of Multiple Drugs of Abuse.” *The AAPS Journal* 7 (2): E353–60.

Valentine, J. D., J. S. Hokanson, S. G. Matta, and B. M. Sharp. 1997. “Self-Administration in Rats Allowed Unlimited Access to Nicotine.” *Psychopharmacology* 133 (3): 300–304.

Vialou, Vincent, Jian Feng, Alfred J. Robison, Stacy M. Ku, Deveroux Ferguson, Kimberly N. Scobie, Michelle S. Mazei-Robison, Ezekiell Mouzon, and Eric J. Nestler. 2012. “Serum Response Factor and cAMP Response Element Binding Protein Are Both Required for Cocaine Induction of ΔFosB.” *The Journal of Neuroscience: The Official Journal of the Society for Neuroscience* 32 (22): 7577–84.

Yan, Z., J. Feng, A. A. Fienberg, and P. Greengard. 1999. “D(2) Dopamine Receptors Induce Mitogen-Activated Protein Kinase and cAMP Response Element-Binding Protein Phosphorylation in Neurons.” *Proceedings of the National Academy of Sciences of the United States of America* 96 (20): 11607–12.

Yao, Yun, Ge Gao, Kai Liu, Xin Shi, Mingxiu Cheng, Yan Xiong, and Sen Song. 2021. “Projections from D2 Neurons in Different Subregions of Nucleus Accumbens Shell to Ventral Pallidum Play Distinct Roles in Reward and Aversion.” *Neuroscience Bulletin* 37 (5): 623–40.

Yu, Guoliang, and Burt M. Sharp. 2015. “Basolateral Amygdala and Ventral Hippocampus in Stress-Induced Amplification of Nicotine Self-Administration during Reacquisition in Rat.” *Psychopharmacology* 232 (15): 2741–49.

Zhu, Shu-Hong, Madeleine Lee, Yue-Lin Zhuang, Anthony Gamst, and Tanya Wolfson. 2012. “Interventions to Increase Smoking Cessation at the Population Level: How Much Progress Has Been Made in the Last Two Decades?” *Tobacco Control* 21 (2): 110–18.

Acknowledgments This research was supported by research funds provided to a Distinguished Professor at the University of Tennessee.

Conflict of interest: None

Figures

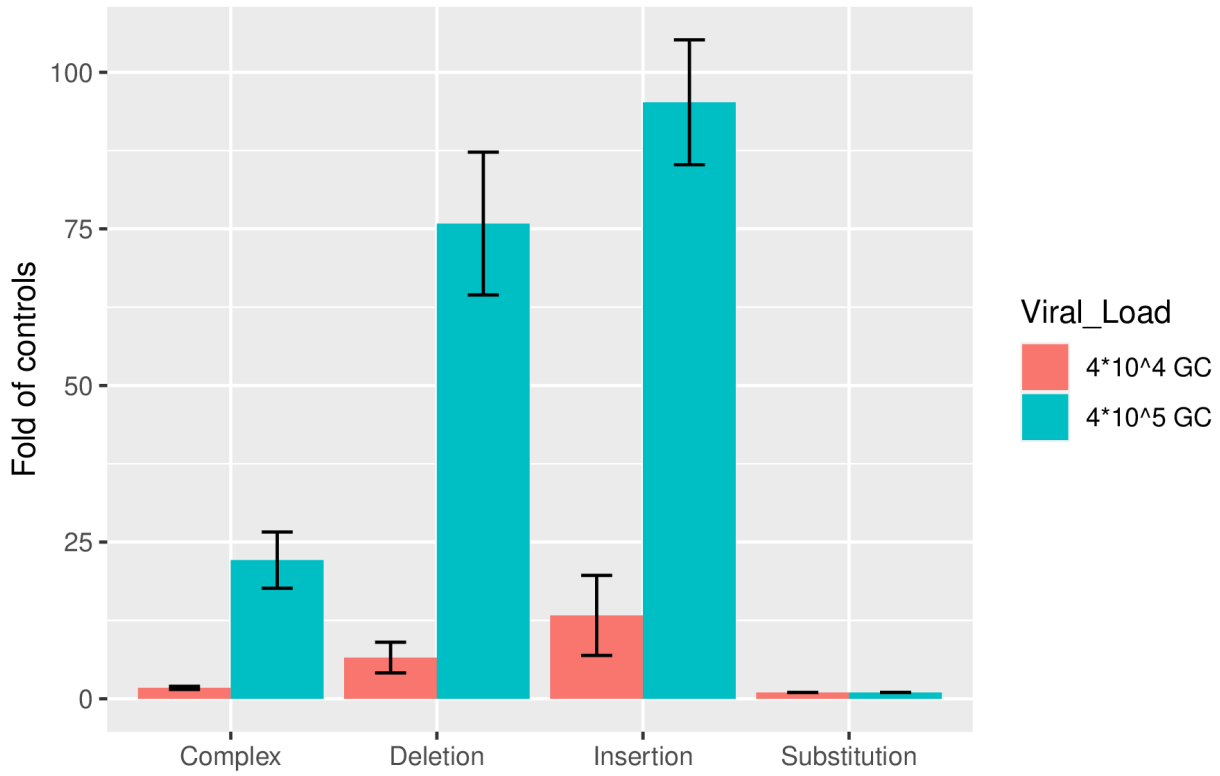

Figure 1. Mutations detected in medial NAcs treated with a gRNA to PDE4B.
NAcs were microinjected *in vivo* with pAAV8-hSyn-Kozak-iCre-P2A-mClover3 -U6-gRNA or control construct and tissue was obtained 45 days later, following completion of a trial of nicotine SA through FR7. The fold-change vs. control depended on the dose of AAV injected.

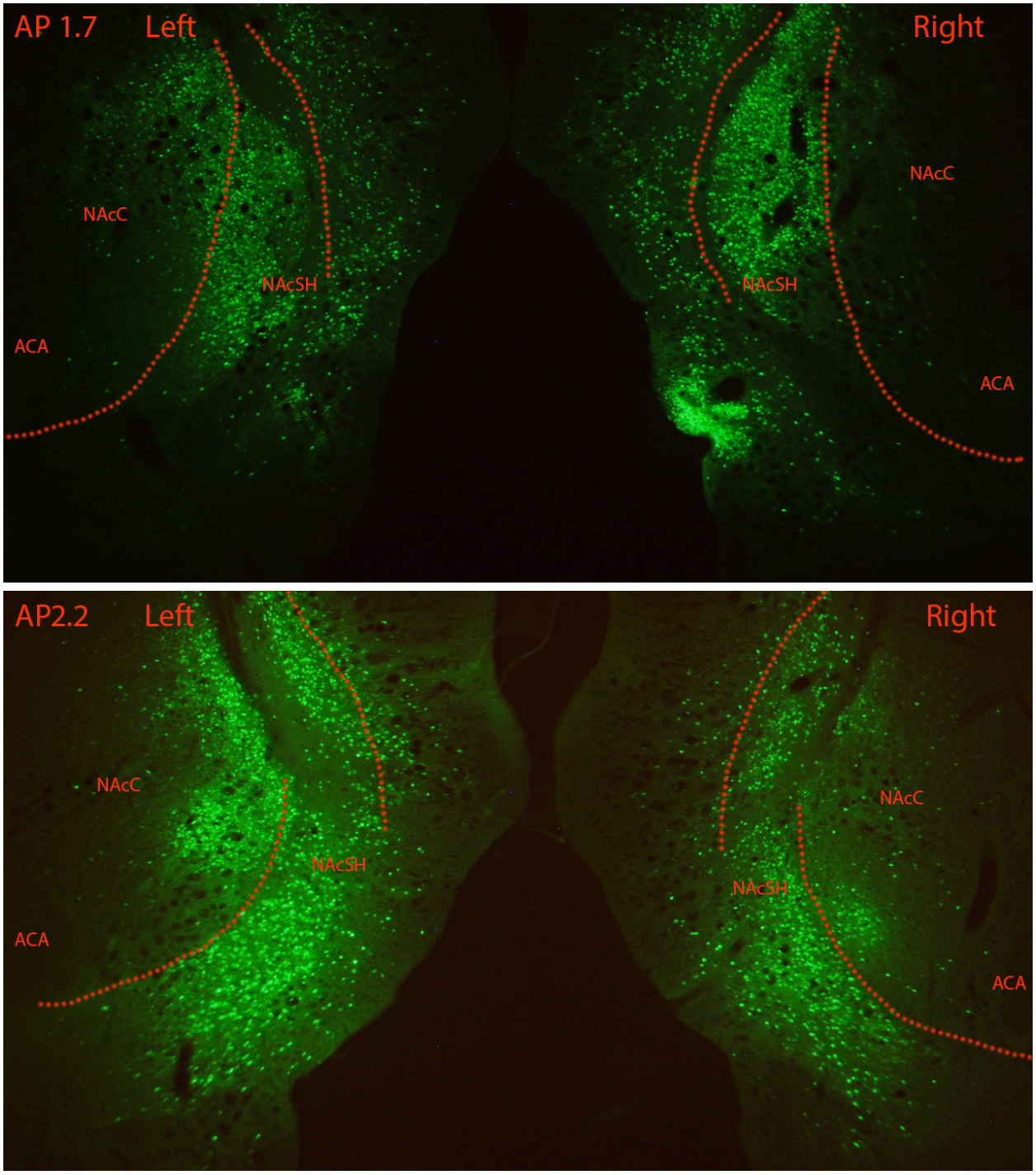

Figure 2. Representative photomicrographs of mClover fluorescence in NAcs from one rat brain at AP 1.7 and 2.2.
Neural fluorescence in nuclei was detected 45 days after injection of the AAV-PDE4B-gRNA construct.

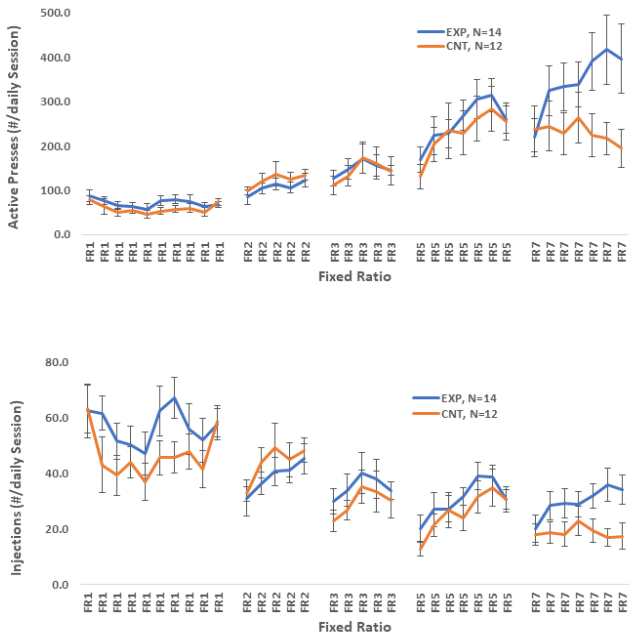

Figure 3. Operant nicotine SA under an increasing fixed ratio (FR) schedule in rats treated with an AAV-PDE4B-gRNA (EXP) or control (CNT) constructs.

Rats had access to nicotine SA everyday for 23 hours/day in operant chambers equipped with active and inactive levers. Daily active lever presses (upper panel) and nicotine injections (lower panel) are shown according to FR schedule for both treatment groups. The average daily active press elicited by each rat during the final 3 days of FR7: EXP = 403.1 ± 68.9 (mean ± SE; n=14) vs. CNT = 211.3 ± 36.5 (n=12) (P=0.028); nicotine infusions, EXP = 33.9 ± 4.6 vs. CNT = 17.9±3.7 (P=0.0134). Analysis of all 7-daily FR7 responses for EXP vs CNT (repeated measures 2-way ANOVA): showed a significant treatment effect on injection (P=0.046), but not on active presses (P=0.081).

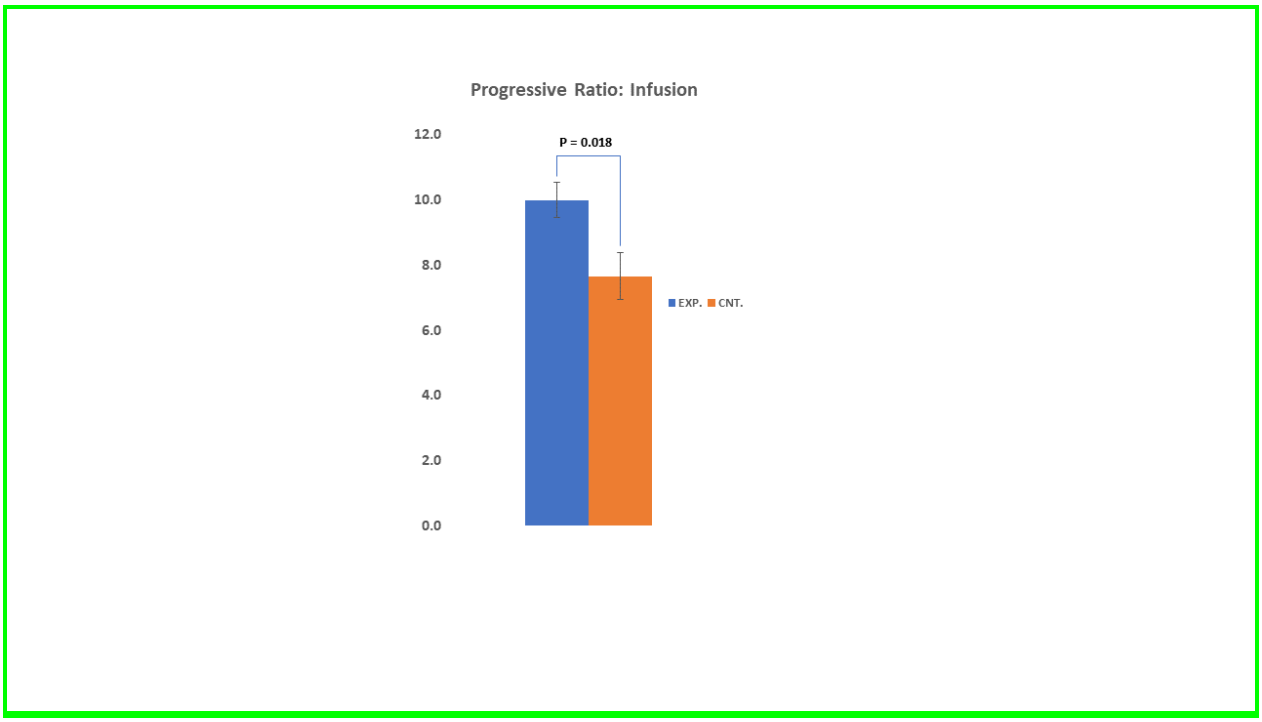

Figure 4. Progressive ratio (PR) test in rats treated (EXP) with an AAV-PDE4B-gRNA or control construct (CNT).
In the PR test, conducted a day after completion of nicotine SA at FR7, the cumulative infusions obtained by the two treatment groups were: EXP = 10.0 ± 0.5 (mean ± SE; n=14) vs. CNT = 7.7 ± 0.7 (n=12) (P=0.018; unpaired T-test, 2-tailed).

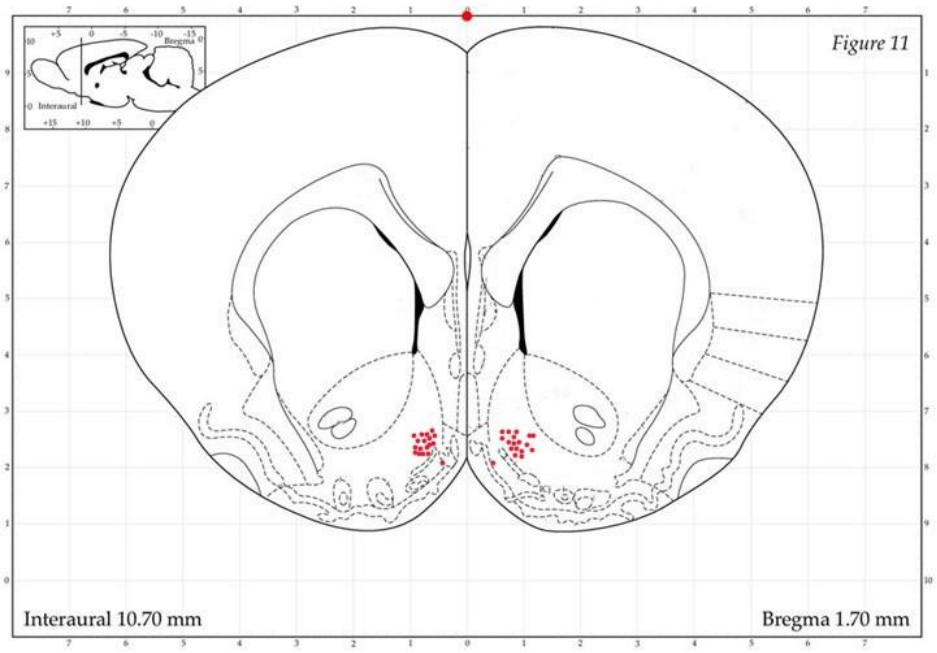

Figure 5. A schematic showing the NAcs locations of all injection needle tips used to administer MR-L2 to rats on day 6 of the 7-day FR3 schedule. The brain section was adapted from the rat brain atlas of Paxinos and Watson (1997).

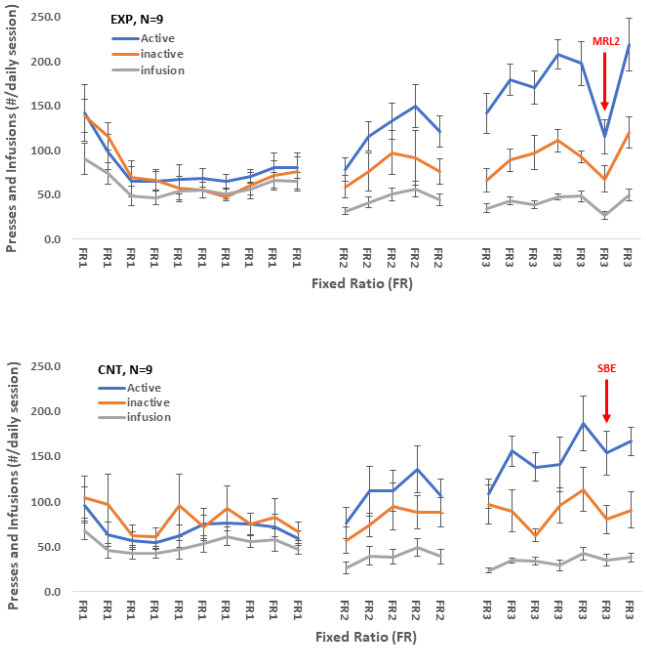

Figure 6. Operant nicotine SA under an increasing fixed ratio (FR) schedule in rats treated with MR-L2 (EXP) or vehicle (CNT) at FR3.

Active and inactive presses and infusions are shown for EXP (upper panel: MR-L2 $2x10^{-4}$ M, 300nl/side) and CNT (lower panel: DMSO-SBE) groups. Comparing days 3-6, MR-L2 significantly reduced active presses on day 6 in EXP, but not in CNT: effect of treatment, F=0.49, P=0.5; day, $F_{1,17}$=10.35, P=0.0054; treatment x day, $F_{1,17}$=9.60, P=0.0069 (repeated measures 2-way ANOVA). *Post-hoc* analysis showed that active presses on days 3-5 were greater than day 6 in the EXP (P=0.029, Tukey), but not CNT (P=0.99) group. Nicotine infusions were significantly reduced by MR-L2 on day 6: treatment, F=0.69, P=0.42; day, $F_{1,17}$=9.28, P=0.0077; treatment x day, $F_{1,17}$=9.44, P=0.0073; infusions on days 3-5 > day 6 in EXP (P=0.033; Tukey), but not CNT (P=0.99).

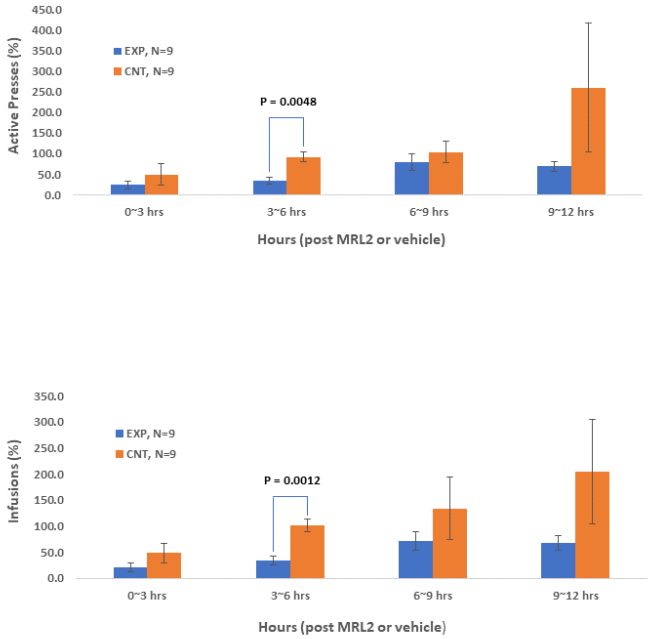

Figure 7. The effect of MR-L2 on nicotine SA at FR3 depends on time post-treatment. Total active presses elicited or infusions (shown in Fig. 6) were binned in time intervals 0-3, 3-6, 6-9, and 9-12 hours after administration of MR-L2 into NAcs bilaterally. These data were normalized by the average value for the corresponding time bins recorded on days 3-5. Significant effects of MR-L2 (EXP) vs. vehicle (CNT) on active presses (upper panel) and infusions (lower panel) occurred between 3-6 hours after dosing: treatment at 3-6 hours post MR-L2, P=0.0048 and 0.0012, respectively; all other time bins, P>0.05 (P values adjusted for multiple testing).

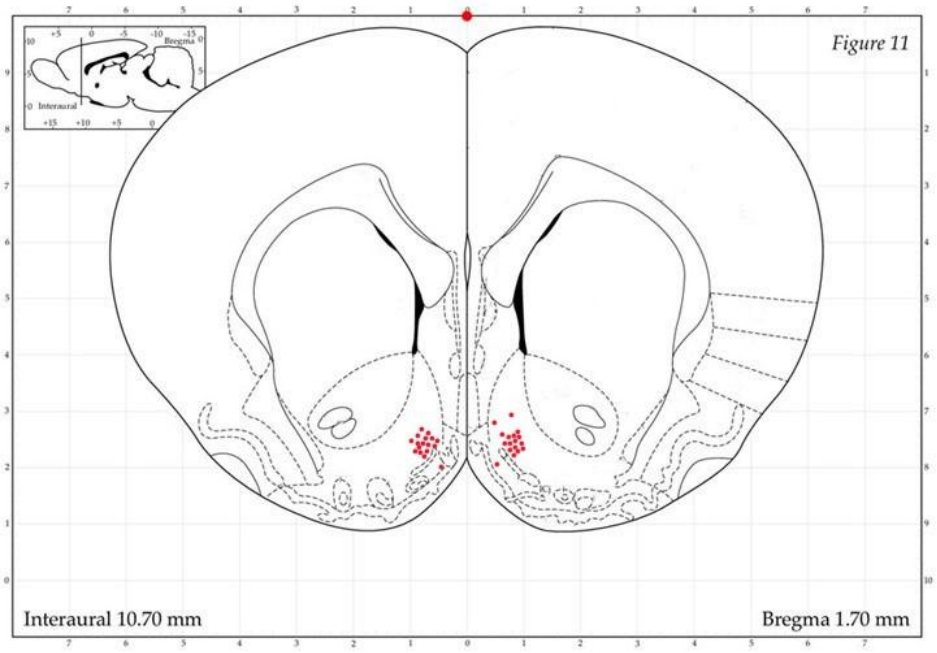

Figure 8. A schematic showing the NAcs locations of all injection needle tips used to administer MR-L2 to rats on day 8 of the 9-day FR5 schedule. The brain section was adapted from the rat brain atlas of Paxinos and Watson (1997).

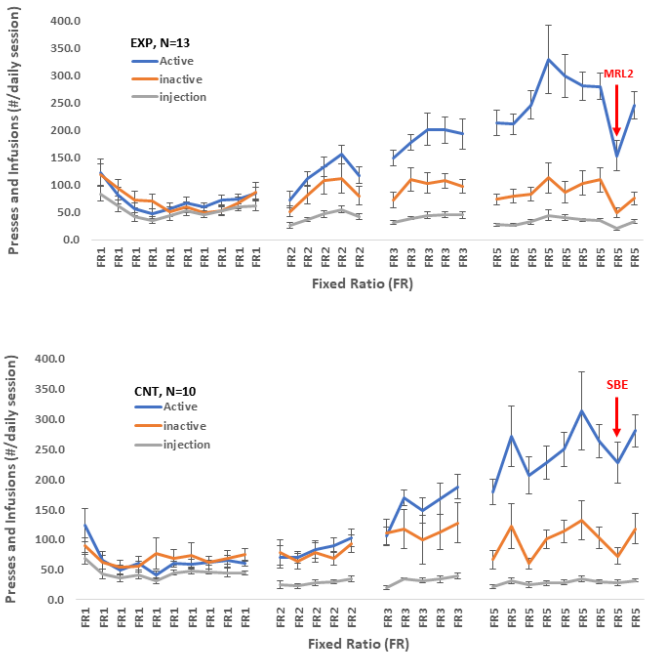

Figure 9. Operant nicotine SA under an increasing fixed ratio (FR) schedule in rats treated on day 8 with MR-L2 (EXP) or vehicle (CNT) at FR5.
Active and inactive presses and infusions are shown for EXP (upper panel: MR-L2 $2x10^{-4}$ M, 300nl/side) and CNT (lower panel: DMSO-SBE) groups. Comparing days 5-8, MR-L2 significantly reduced active presses on day 8 in EXP, but not in CNT: treatment, F=0.014, P=0.91; day, F=22.61, P=8.58e-05; treatment x day, F=2.06, P=0.16 (repeated measures 2-way ANOVA). Nicotine infusions were significantly reduced by MR-L2 on day 8: treatment, F=0.088, P=0.77; day, F=16.22, P=0.00053; treatment x day, F=3.10, P=0.091 *Post-hoc* analysis showed: active presses on days 5-7 > day 8 in the EXP (P=0.0071, Tukey), but not CNT (P=0.43) group; infusions on days 5-7 > day 8 in EXP (P=0.0029; Tukey), but not CNT (P=0.65).

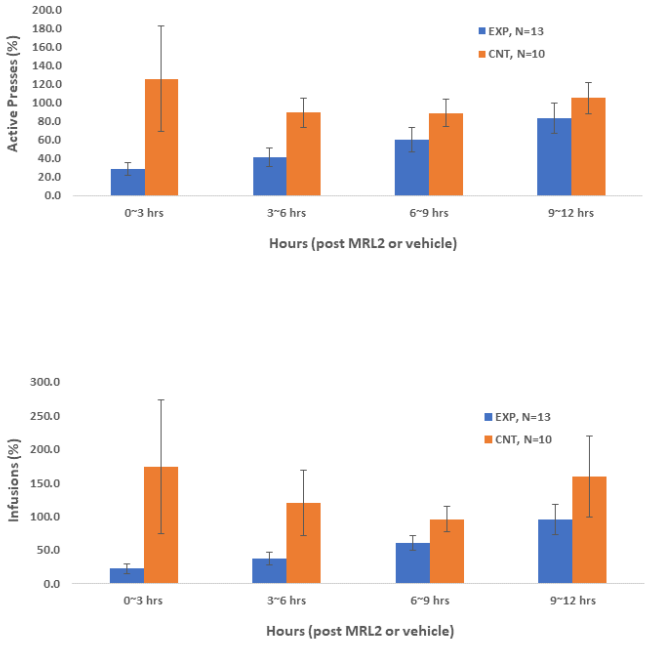

Figure 10. The effect of time post-MR-L2 infusion on day 8 nicotine SA at FR5.
Total active presses elicited or infusions (shown in Fig. 9) were binned in time intervals 0-3, 3-6, 6-9, and 9-12 hours after administration of MR-L2 into NAcs bilaterally. These data were normalized by the average value for the corresponding time bins recorded on days 5-7. A significant effect of treatment group was found for both active presses (upper panel) and infusions (lower panel): $F=5.37$, $P=0.030$ and $F=4.84$, $P=0.038$, respectively (repeated measures 2-way ANOVA); neither bin time nor treatment x time were significant ($P > 0.05$), nor were *post-hoc* tests.